

SUPPLEMENTARY MATERIALS

Discovery of a novel tetrapeptide against Influenza A virus: rational design, synthesis, bioactivity evaluation and computational studies.

Maria Carmina Scala^a, [§], Mariangela Agamennone^b, [§], Agostina Pietrantoni, ^{c,d} Veronica Di Sarno,^a Alessia Bertamino,^a Fabiana Superti^c, Pietro Campiglia^a and Marina Sala^{a,}*

^aDepartment of Pharmacy, University of Salerno, Via Giovanni Paolo II 132, 84084, Fisciano (SA), Italy

^bDepartment of Pharmacy, University “G. d’Annunzio” of Chieti-Pescara, Via dei Vestini 31, 66100, Chieti, Italy

^cNational Centre for Innovative Technologies in Public Health, National Institute of Health, Viale Regina Elena 299, 00161, Rome, Italy

^dCore Facilities, National Institute of Health, Viale Regina Elena 299, 00161, Rome, Italy

* Corresponding author: msala@unisa.it; Tel.: 089968148

[§] These authors contributed equally to this work

Table of contents:

Supplementary schemes and figures:

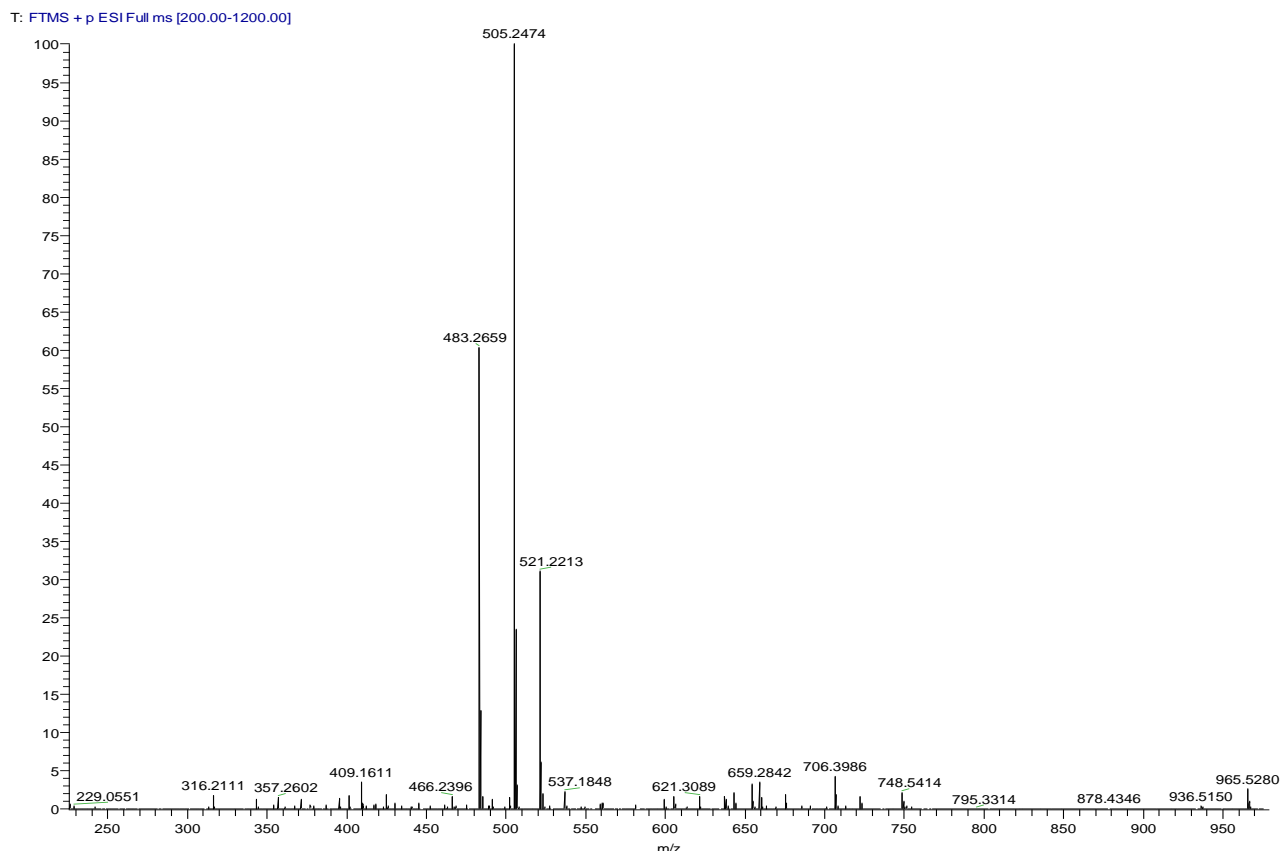
Table S1:	Analytical data of peptides 1-10	S2
Figure S1-S8:	HRMS spectra and HPLC chromatograms of peptide 3-10	S2
Figure S9-S15:	Sensorgrams of peptides 3, 5-10	S10
Figure S16-S19:	MST binding curves of peptides 2, 3, 5-10	S13
Table S2:	Swiss-Model data of homology models	S14
Table S3:	Score values obtained for the best homology models	S15
Figure S20:	Ramachandran Plots of HA homology models	S15
Figure S21:	Alignment of HA sequences of A/Parma and A/Roma H1N1 strains	S16
Figure S22:	Docked poses of peptide 2	S17
Figure S23:	Superposition of the complex of HA:sialic acid with docked pose of SAHS ...	S18

Table S1. Analytical data of peptides **3-10**.

Pep.	Sequence	HPLC k ^a	HRMS
1^a	SKHS	4.68	499.26235
3	AKHS	1.10	483.2659
4	SAHS	0.54	443.1667
5	SKAS	1.85	434.2055
6	SKHA	4.37	483.2654
2^a	SLDC	3.93	477.18970
7	ALDC	5.67	462.2003
8	SADC	3.50	436.1484
9	SLAC	5.16	434.2050
10	SLDA	5.93	446.2235

^ak'=[(peptide retention time-solvent retention time)/solvent retention time].

Supplementary figures of Mass spectrometry and HPLC of peptides used in the study



Datafile Name: Peptide 3

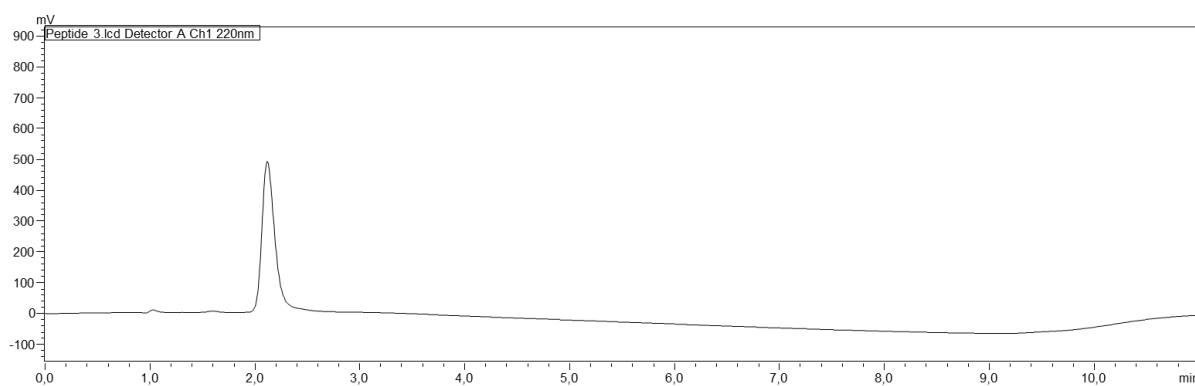


Figure S1. HR-ESI-MS of Peptide 3 ion $[M+H]^+$ and analytical HPLC trace at 220 nm.

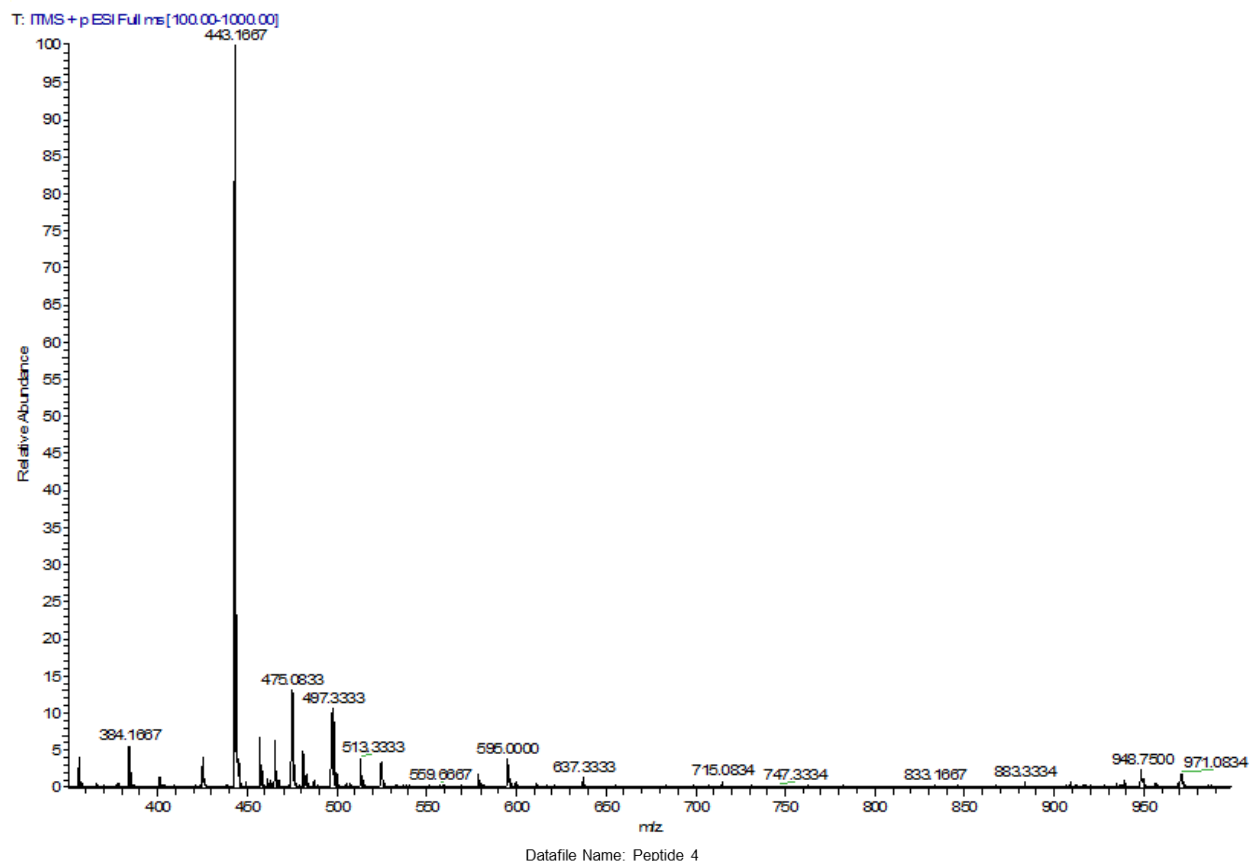


Figure S2. HR-ESI-MS of Peptide 4 ion $[M+H]^+$ and analytical HPLC trace at 220 nm.

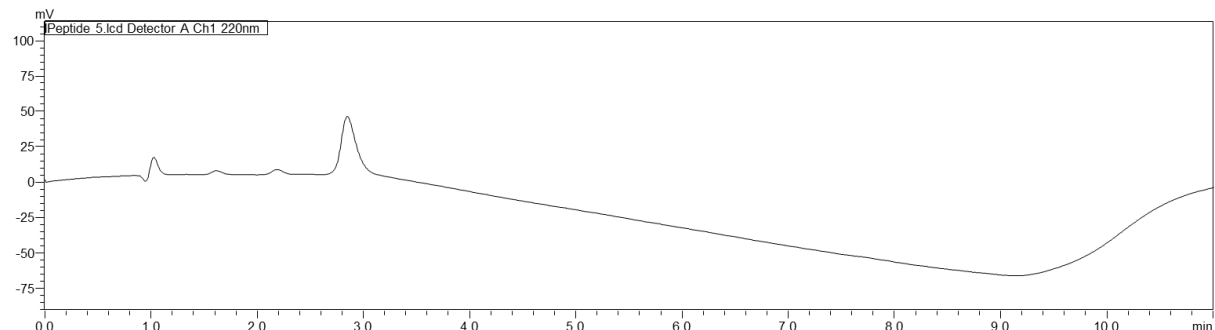
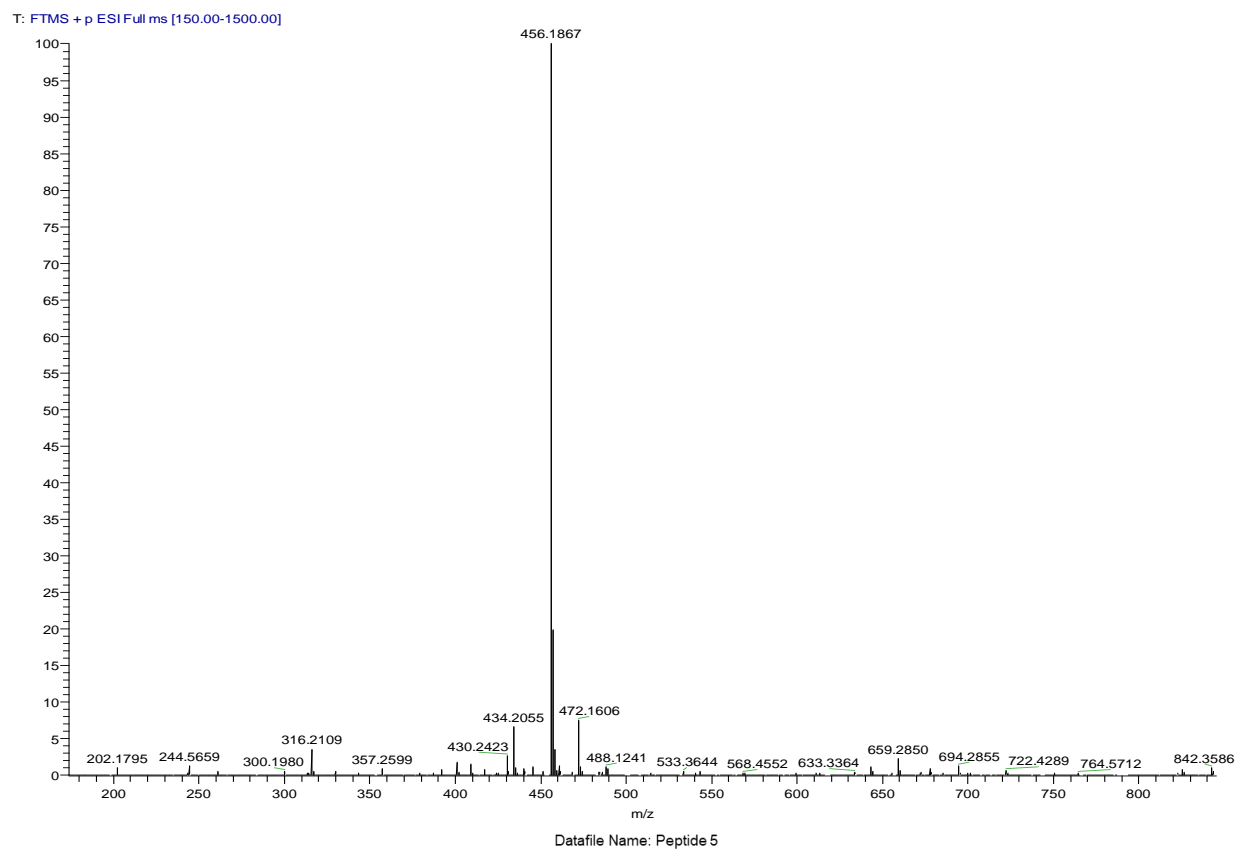


Figure S3. HR-ESI-MS of Peptide 5 ion $[M+H]^+$ and analytical HPLC trace at 220 nm.

T: FTMS + p ESI Full ms [200.00-1200.00]

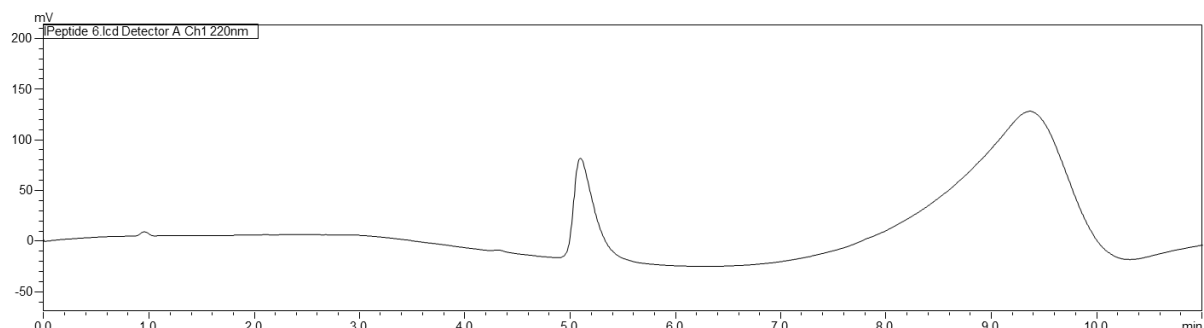
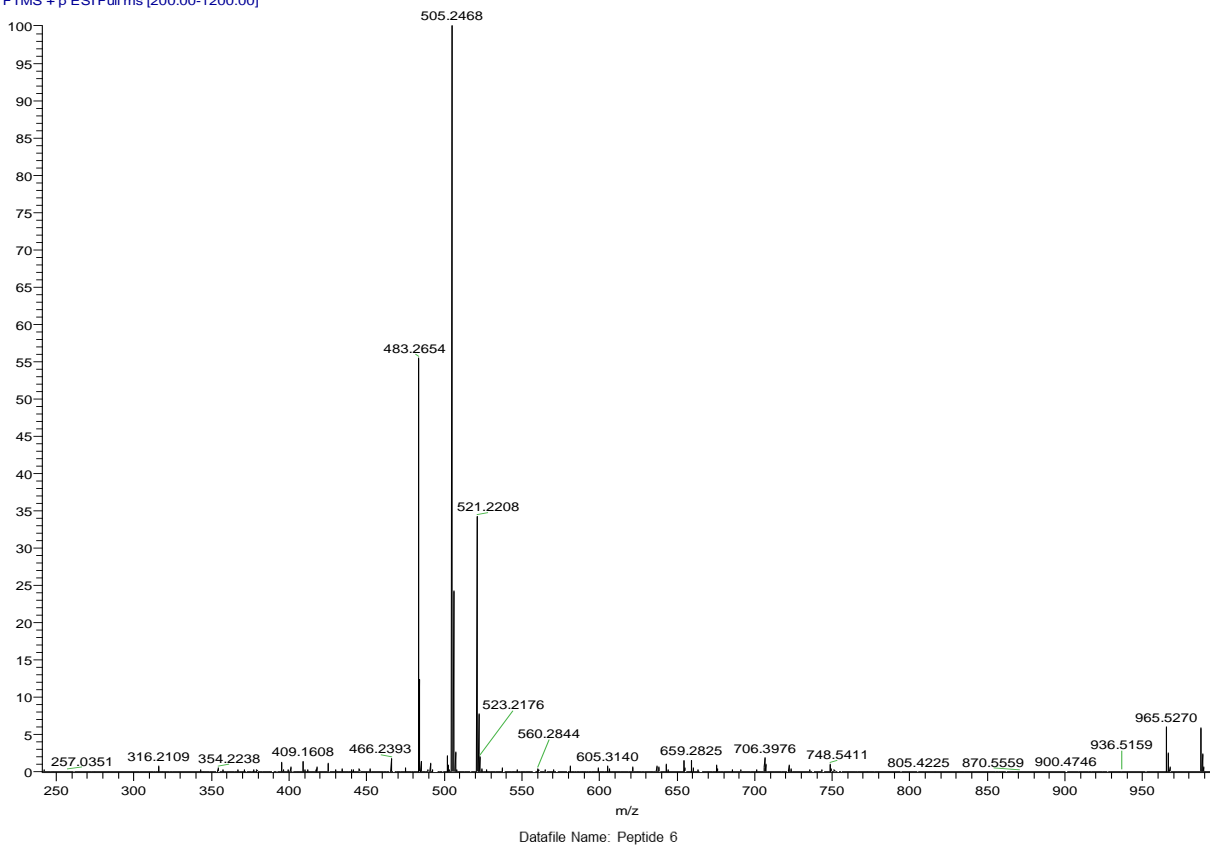


Figure S4. HR-ESI-MS of Peptide **6** ion $[M+H]^+$ and analytical HPLC trace at 220 nm.

T: FTMS + p ESI Full ms [150.00-1500.00]

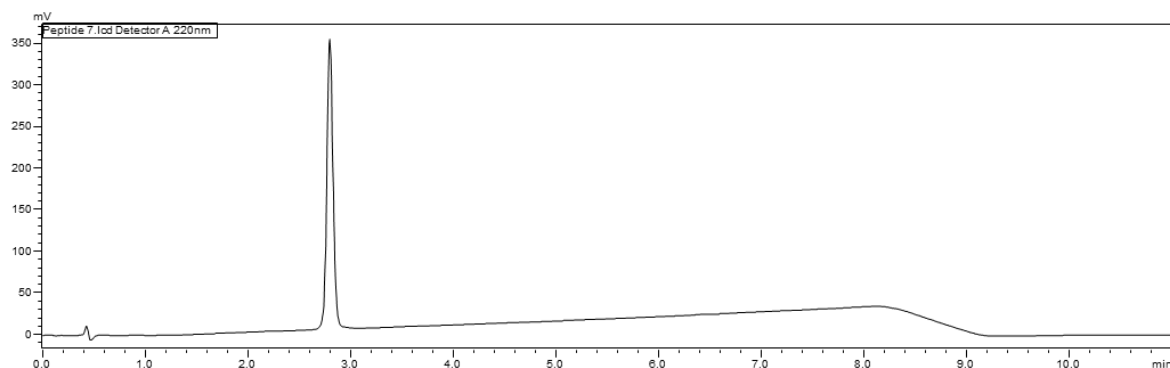
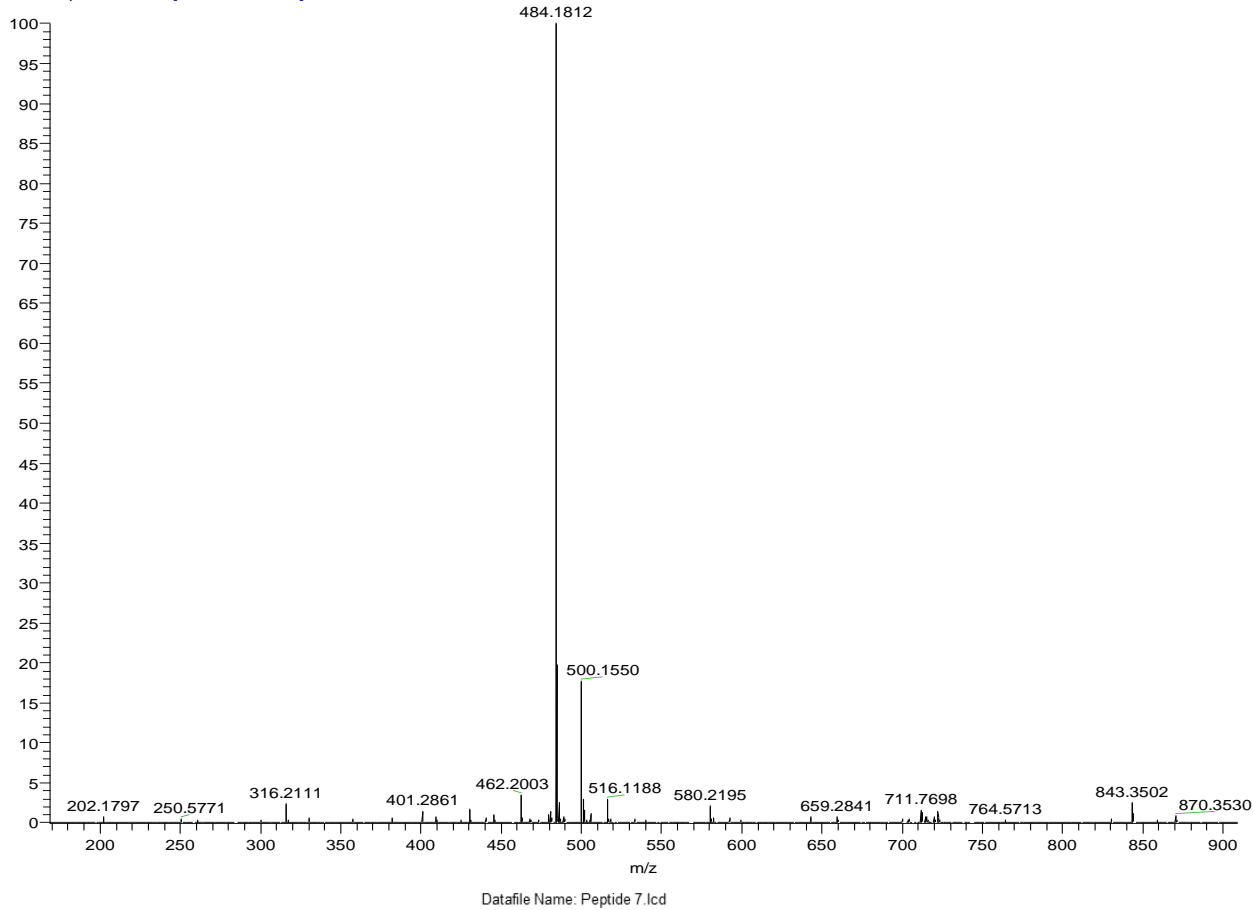
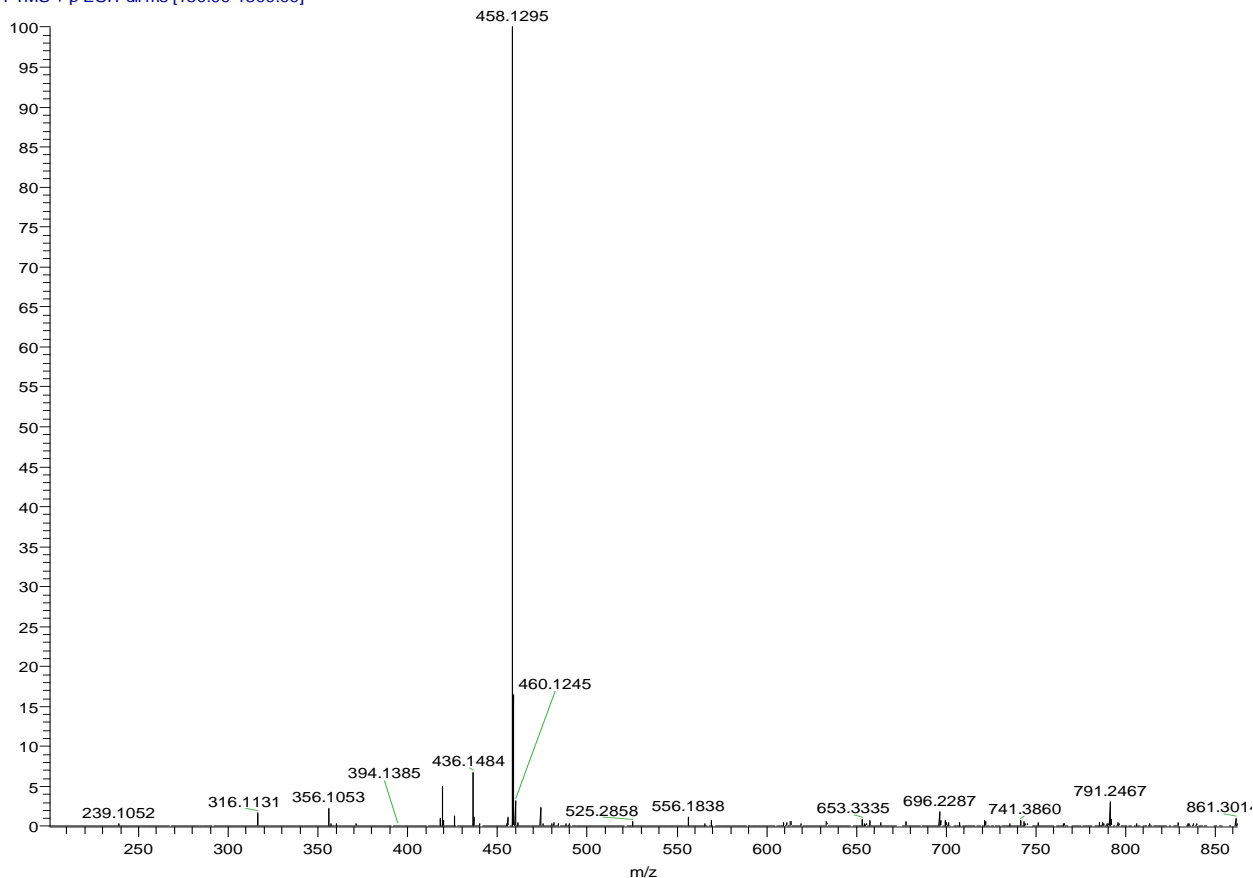


Figure S5. HR-ESI-MS of Peptide 7 ion $[M+H]^+$ and analytical HPLC trace at 220 nm.

T: FTMS + p ESI Full ms [150.00-1500.00]



Datafile Name: Peptide 8.lcd

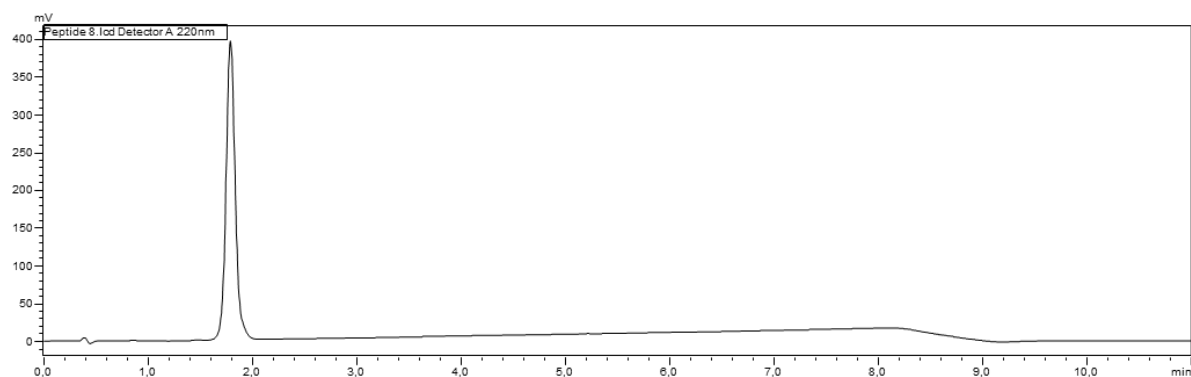


Figure S6. HR-ESI-MS of Peptide **8** ion $[M+H]^+$ and analytical HPLC trace at 220 nm.

T: FTMS + p ESI Full ms [150.00-1500.00]

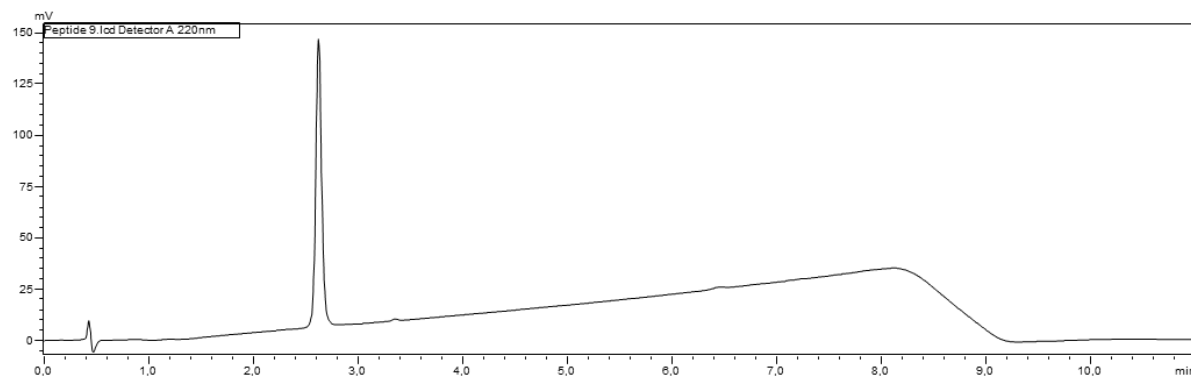
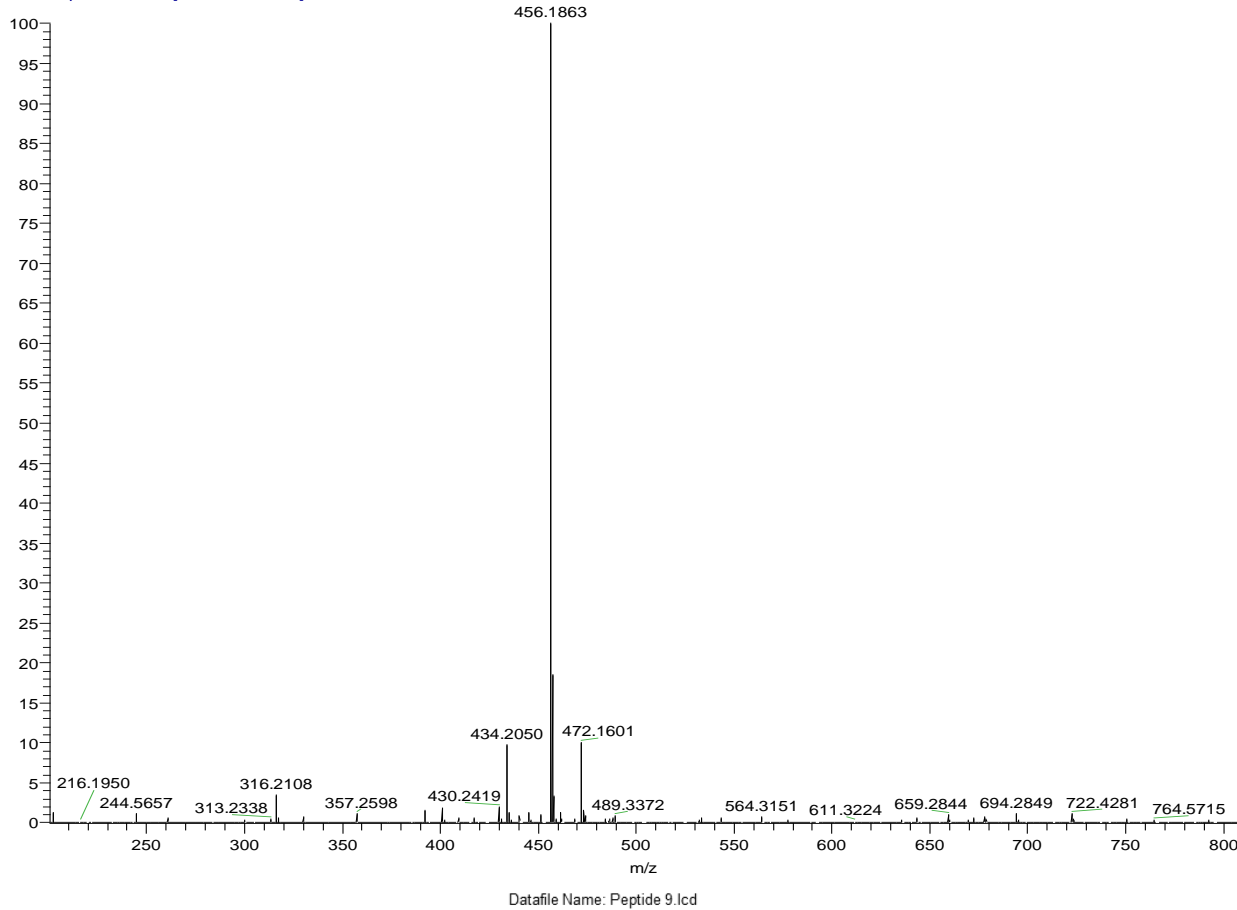


Figure S7. HR-ESI-MS of Peptide **9** ion $[M+H]^+$ and analytical HPLC trace at 220 nm.

T: FTMS + p ESI Full ms [150.00-1500.00]

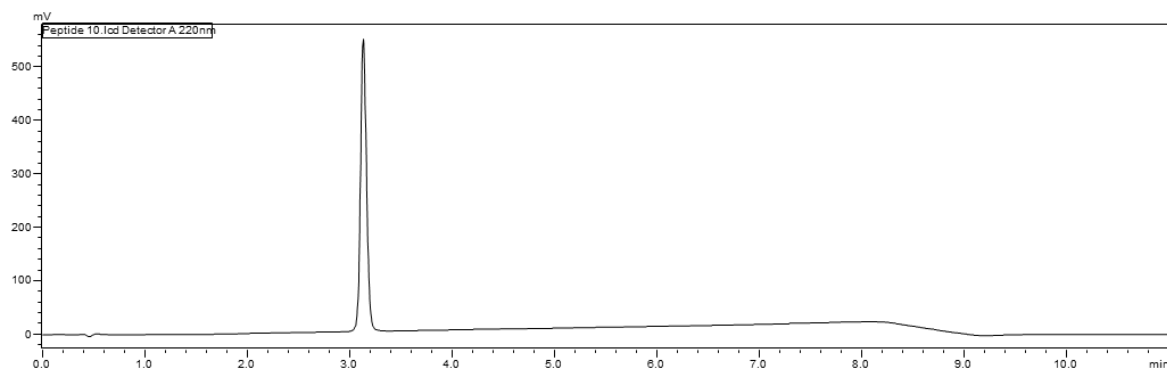
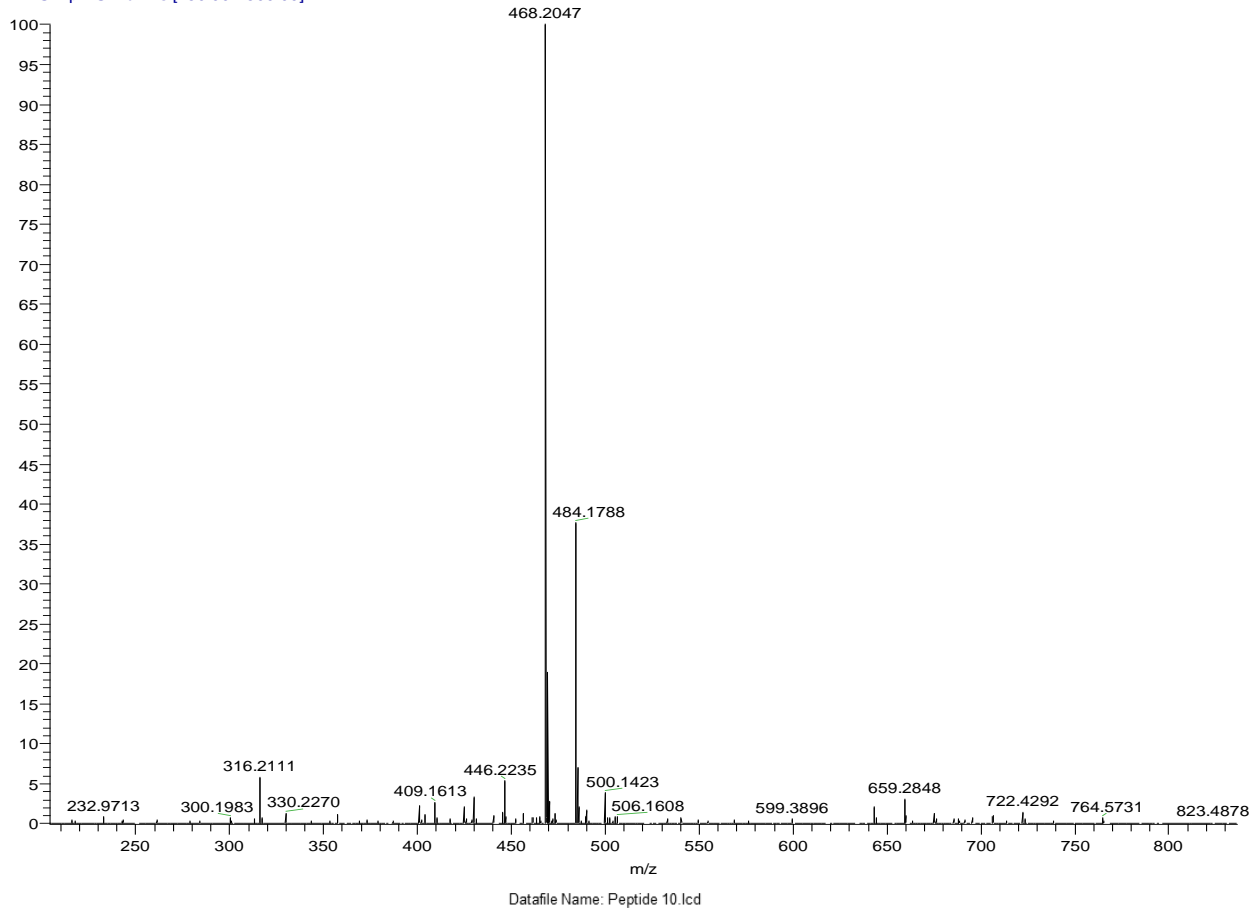


Figure S8. HR-ESI-MS of Peptide **10** ion $[M+H]^+$ and analytical HPLC trace at 220 nm.

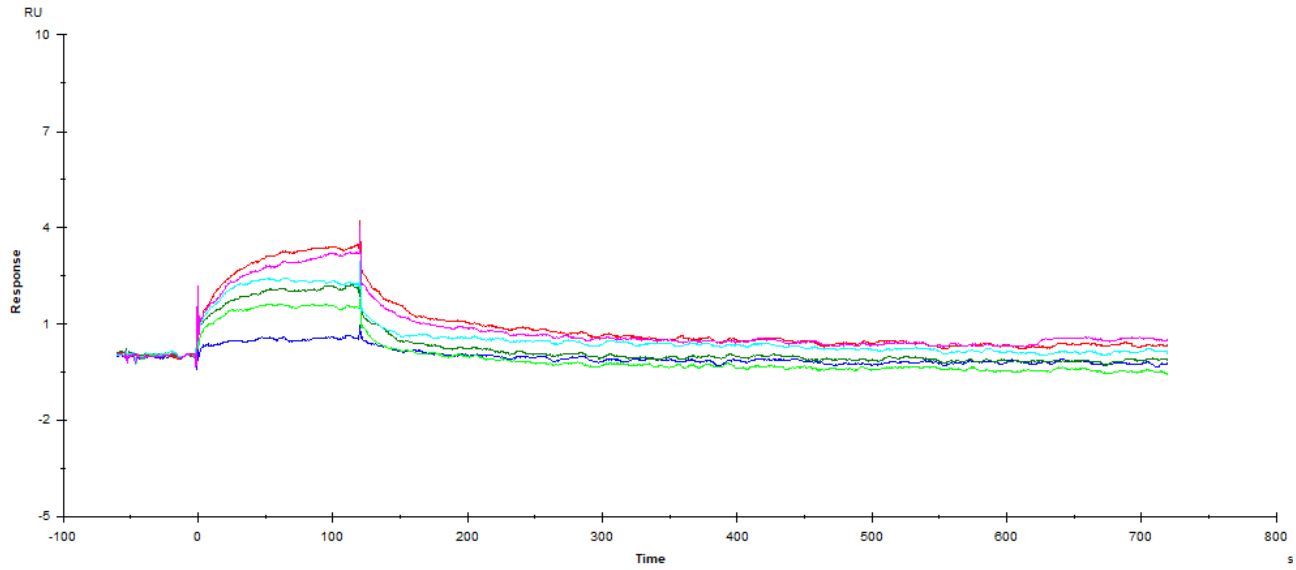


Figure S9. SPR sensorgrams between HA (immobilized on the sensor chip surface) and the compound **3**.

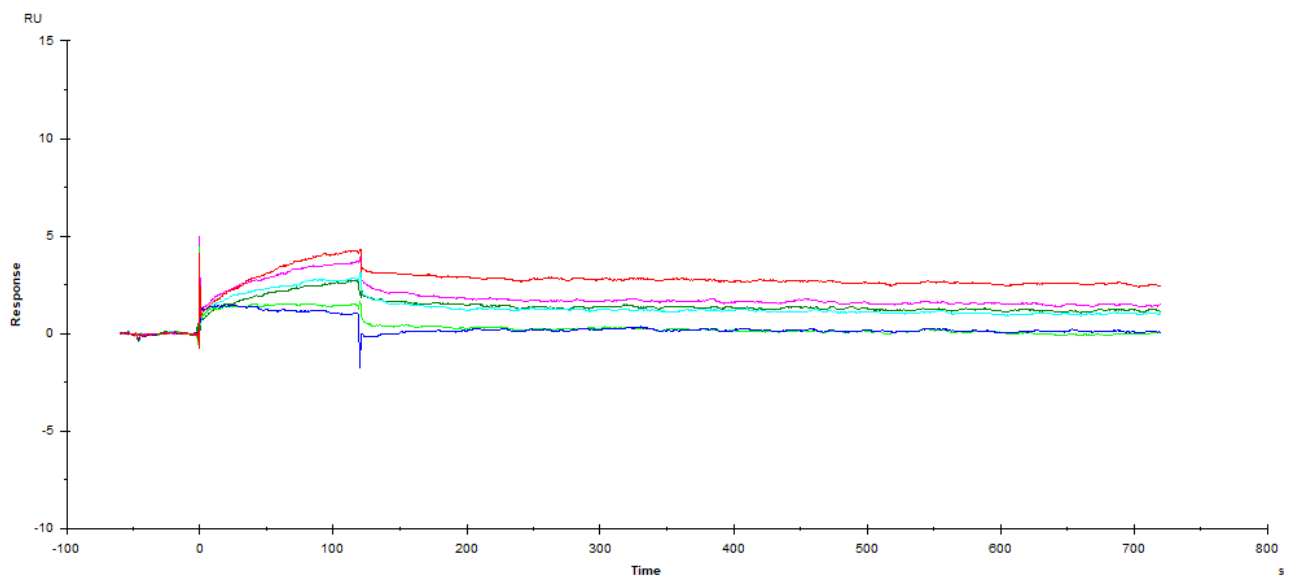


Figure S10. SPR sensorgrams between HA (immobilized on the sensor chip surface) and the compound **5**.

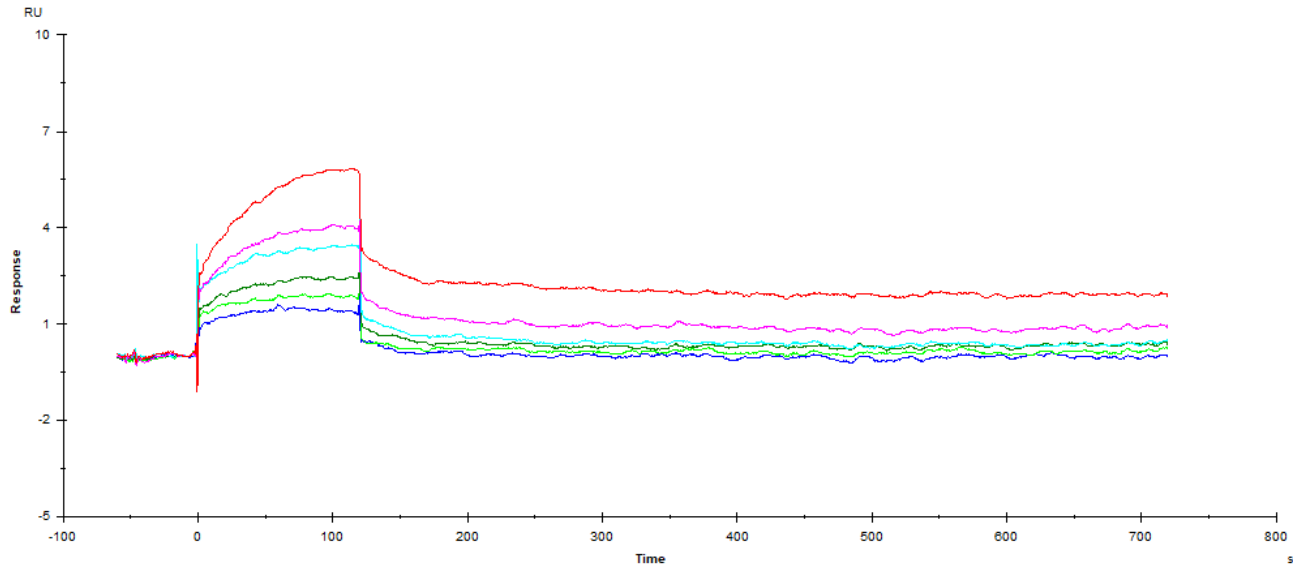


Figure S11. SPR sensorgrams between HA (immobilized on the sensor chip surface) and the compound **6**.

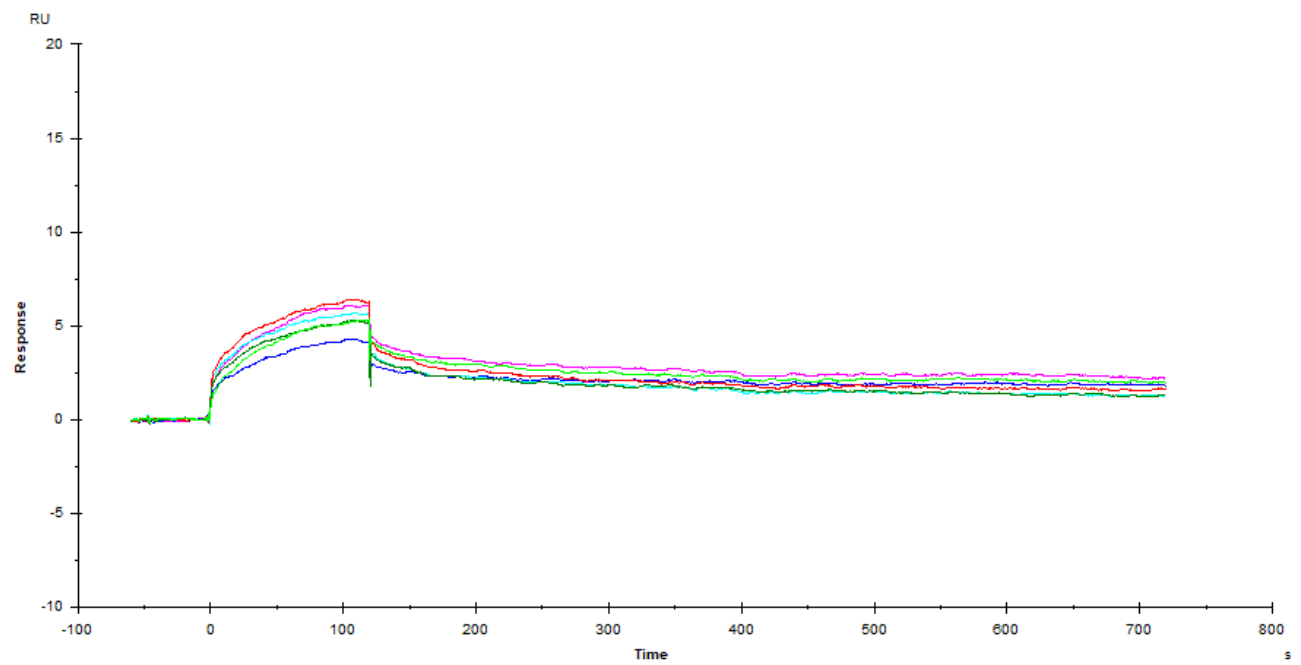


Figure S12. SPR sensorgrams between HA (immobilized on the sensor chip surface) and the compound **7**.

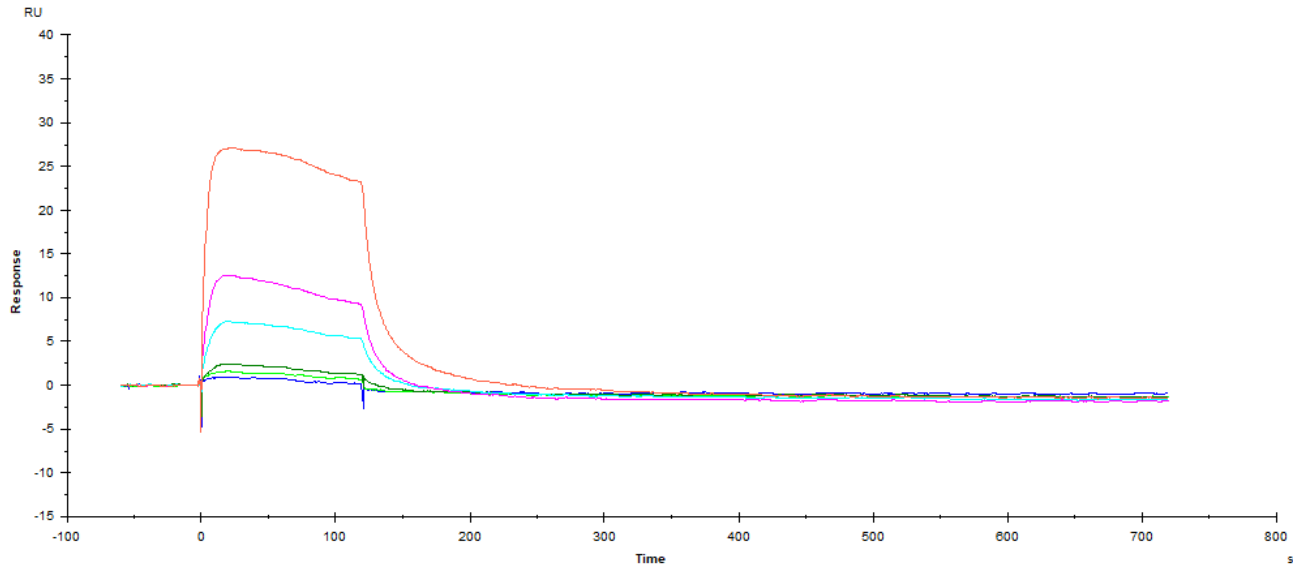


Figure S13. SPR sensorgrams between HA (immobilized on the sensor chip surface) and the compound **8**.

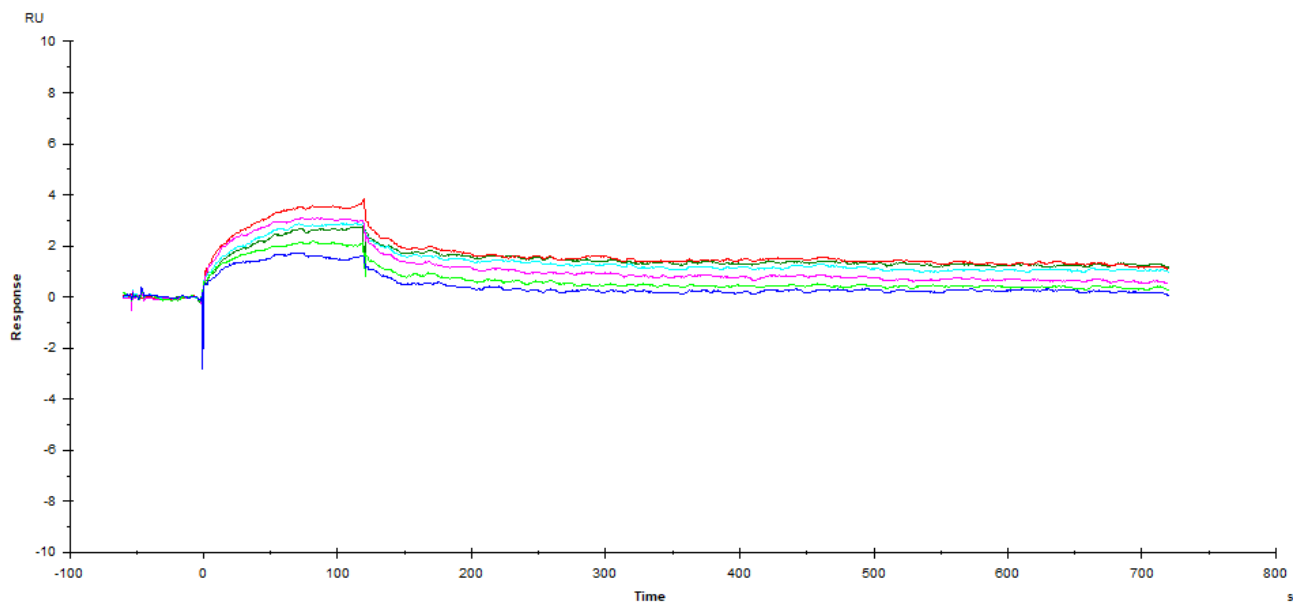


Figure S14. SPR sensorgrams between HA (immobilized on the sensor chip surface) and the compound **9**.

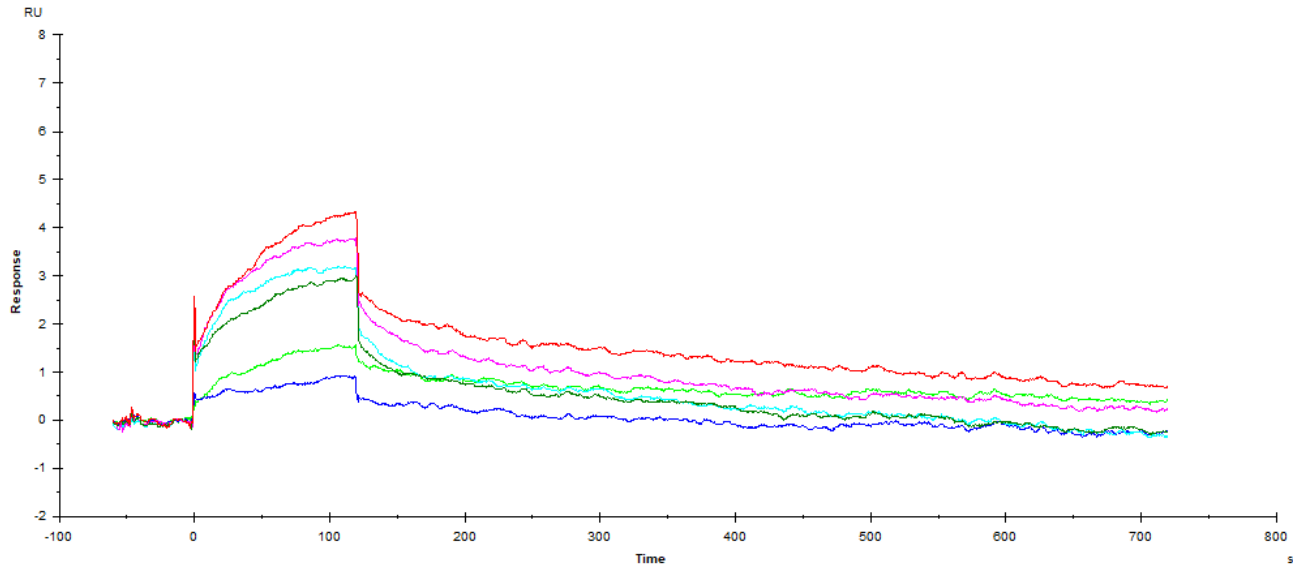


Figure S15. SPR sensorgrams between HA (immobilized on the sensor chip surface) and the compound **10**.

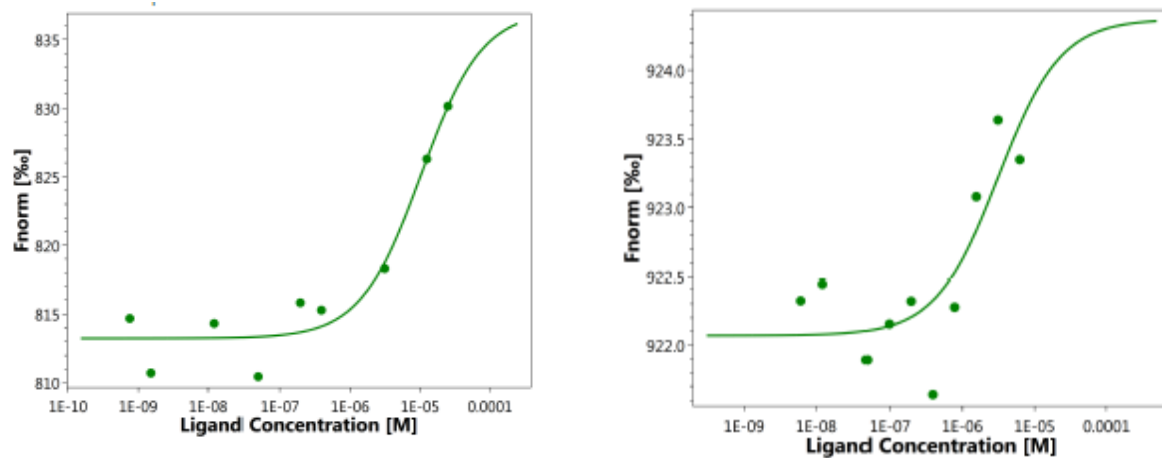


Figure S16. MST binding curve of peptide **2-3** to HA.

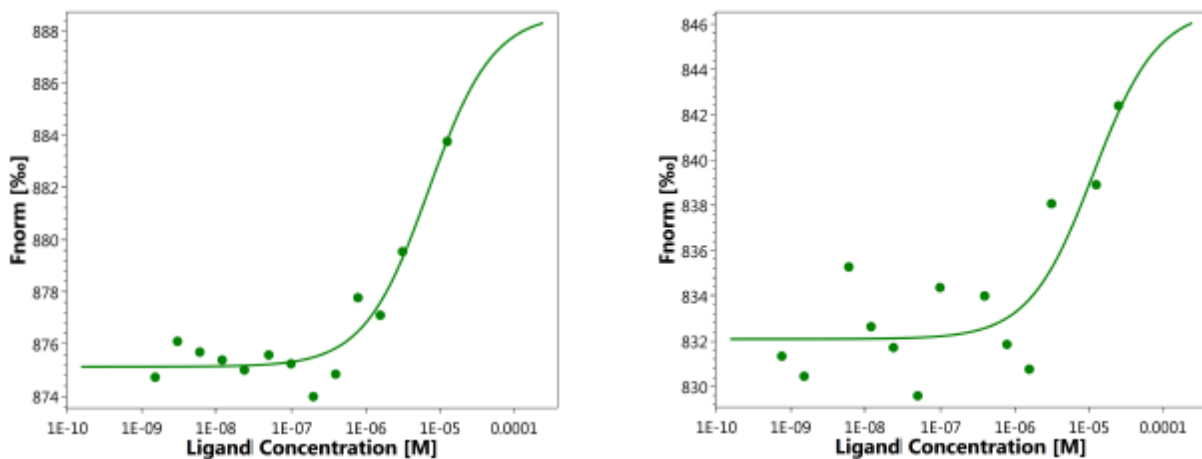


Figure S17. MST binding curve of peptide **5-6** to HA.

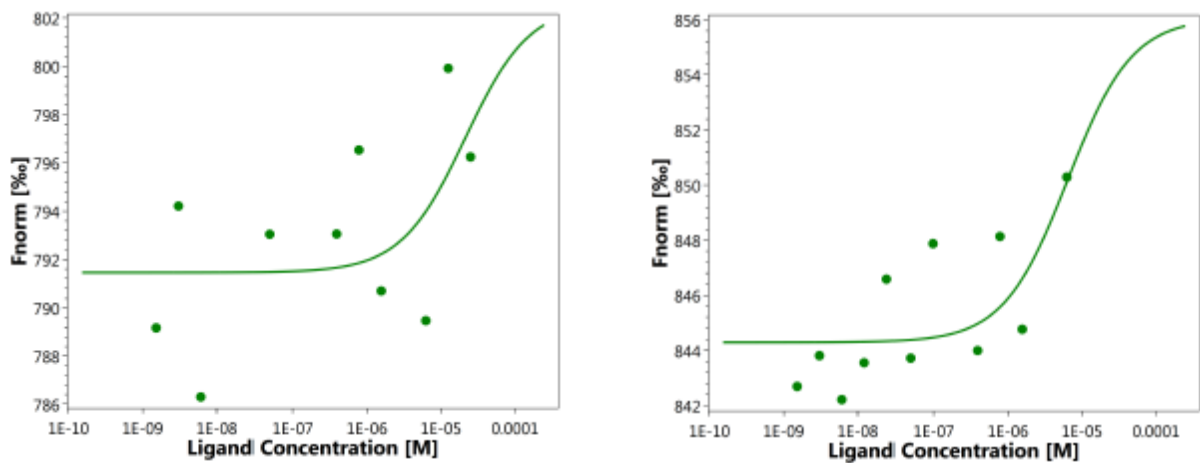


Figure S18. MST binding curve of peptide **7-8** to HA.

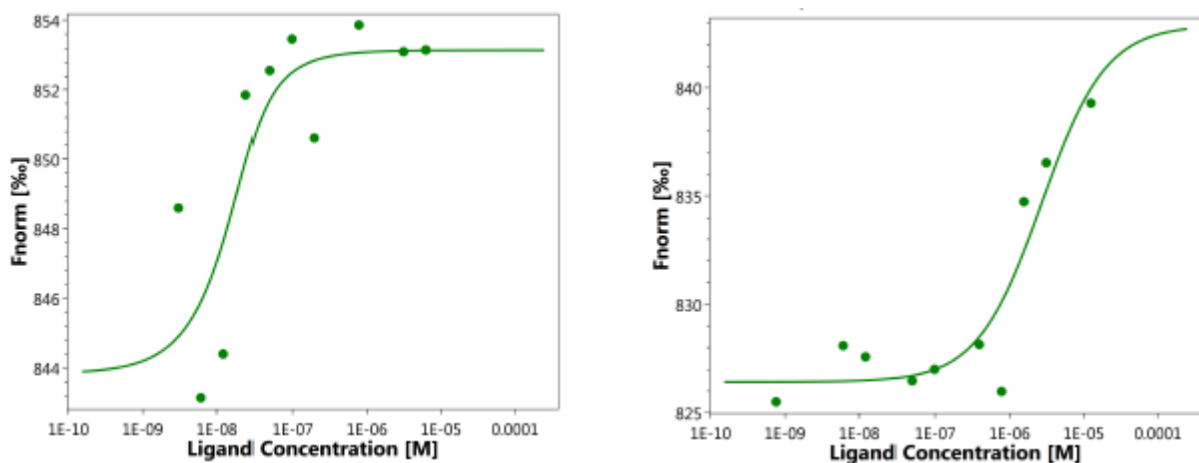


Figure S19. MST binding curve of peptide **9-10** to HA.

Table S2. Best ranking templates used for model generation in Swiss-Model for each HA

Structure	Template	Seq Identity	Oligo-state	QSQE	Found by	Method	Resolution	Seq Similarity	Coverage
Parma_H1N1	6wcr.1	85.92	hetero-3-3-mer	0.95	HHblits	X-ray	2.68 Å	0.58	0.90
Roma_H1N1	6wcr.1	85.95	hetero-3-3-mer	0.96	HHblits	X-ray	2.68 Å	0.58	0.90
Parma_H3N2	6aop.1	98.17	hetero-3-3-mer	0.97	HHblits	X-ray	2.30 Å	0.62	0.90

Table S3. Score values obtained for the best homology models

Structure	Built with	Oligo-state	GMQE	QMEAN
Parma_H1N1	ProMod3 3.1.1	hetero-3-3-mer	0.85	-0.16
Roma_H1N1	ProMod3 3.1.1	hetero-3-3-mer	0.84	-0.08
Parma_H3N2	ProMod3 3.1.1	hetero-3-3-mer	0.90	-0.06

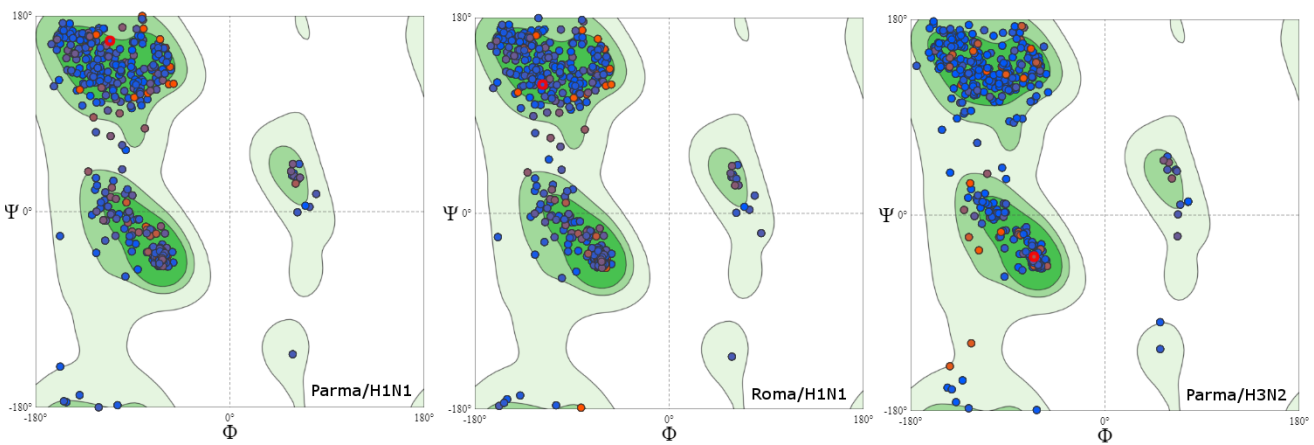


Figure S20. Ramachandran Plots obtained for HA homology models

H1N1_Parma	1	-----STDTVDTVLEKNVTVTHSVNLLENSHNGKLCLKGIA
H1N1_Roma	1	ANNSTDTVDTVLEKNVTVTHSVNLLENSHNGKLCLKGIA
H1N1_Parma	38	PLQLGNCSVAGWILGNPECELLISKESWSYIVEKPNPENG
H1N1_Roma	41	PLQLGNCSVAGWILGNPECELLISKESWSYIVEKPNPENG
H1N1_Parma	78	TCYPGHFADYEELREQLSSVSSFERFEIFPKESSWPNHTV
H1N1_Roma	81	TCYPGHFADYEELREQLSSVSSFERFEIFPKESSWPNHTV
H1N1_Parma	118	TGVS--SCSHNGE NSFYRNLLWLTGKNGLYPNLSKSYANNK
H1N1_Roma	121	TGVS ASCSHNGE SSFYRNLLWLTGKNGLYPNLSKSYANNK
H1N1_Parma	157	EKEVLVLWGVHHPPNI ADQKTLYHTENAYSVVSSHYSRK
H1N1_Roma	161	EKEVLVLWGVHHPPNI GDQKALYHTENAYSVVSSHYSRK
H1N1_Parma	197	FTPEIAKRPKVRDQEGRINYYWTLEPGDTIIFEANGNLI
H1N1_Roma	201	FTPEIAKRPKVRDQEGRINYYWTLEPRDTIIFEANGNLI
H1N1_Parma	237	APRYAFALSRGFSGIINSNAPMDKCDAKCQTPQGAINSS
H1N1_Roma	241	APRYAFALSRGFSGIINSNAPMDKCDAKCQTPQGAINSS
H1N1_Parma	277	LPFQNVHPVTIGECPKYVRSAKLRMVTGLRNIPSGLFGAI
H1N1_Roma	281	LPFQNVHPVTIGECPKYVRSAKLRMVTGLRNIPS----GAI
H1N1_Parma	7	AGFIEGGWTGMVDGWGYHHQNEQGSGYAADQKSTQNAIN
H1N1_Roma	4	AGFIEGGWTGMVDGWGYHHQNEQGSGYAADQKSTQNAIN
H1N1_Parma	47	GITNKVNSVIEKMNTQFTAVGKEFNKLERRMENLNKKVDD
H1N1_Roma	44	GITNKVNSVIEKMNTQFTAVGKEFNKLERRMENLNKKVDD
H1N1_Parma	87	GFIDIWTYNAELLVLENERTLDFHDSNVKNLYEKVSQL
H1N1_Roma	84	GFIDIWTYNAELLVLENERTLDFHDSNVKNLYEKVSQL
H1N1_Parma	127	KNNAKEIGNGCFEFYHKCNDEC MESVKNGTYDYPKYSEES
H1N1_Roma	124	KNNAKEIGNGCFEFYHKCNDEC MESVKNGTYDYPKYSEES
H1N1_Parma	167	KLNRE-----STDTVDTVLEKNVTVTHSVNLLENSHNGKLCL
H1N1_Roma	164	KLNREANNSTDTVDTVLEKNVTVTHSVNLLENSHNGKLCL

Figure S21. Alignment of HA sequences of A/Parma and A/Roma H1N1 strains

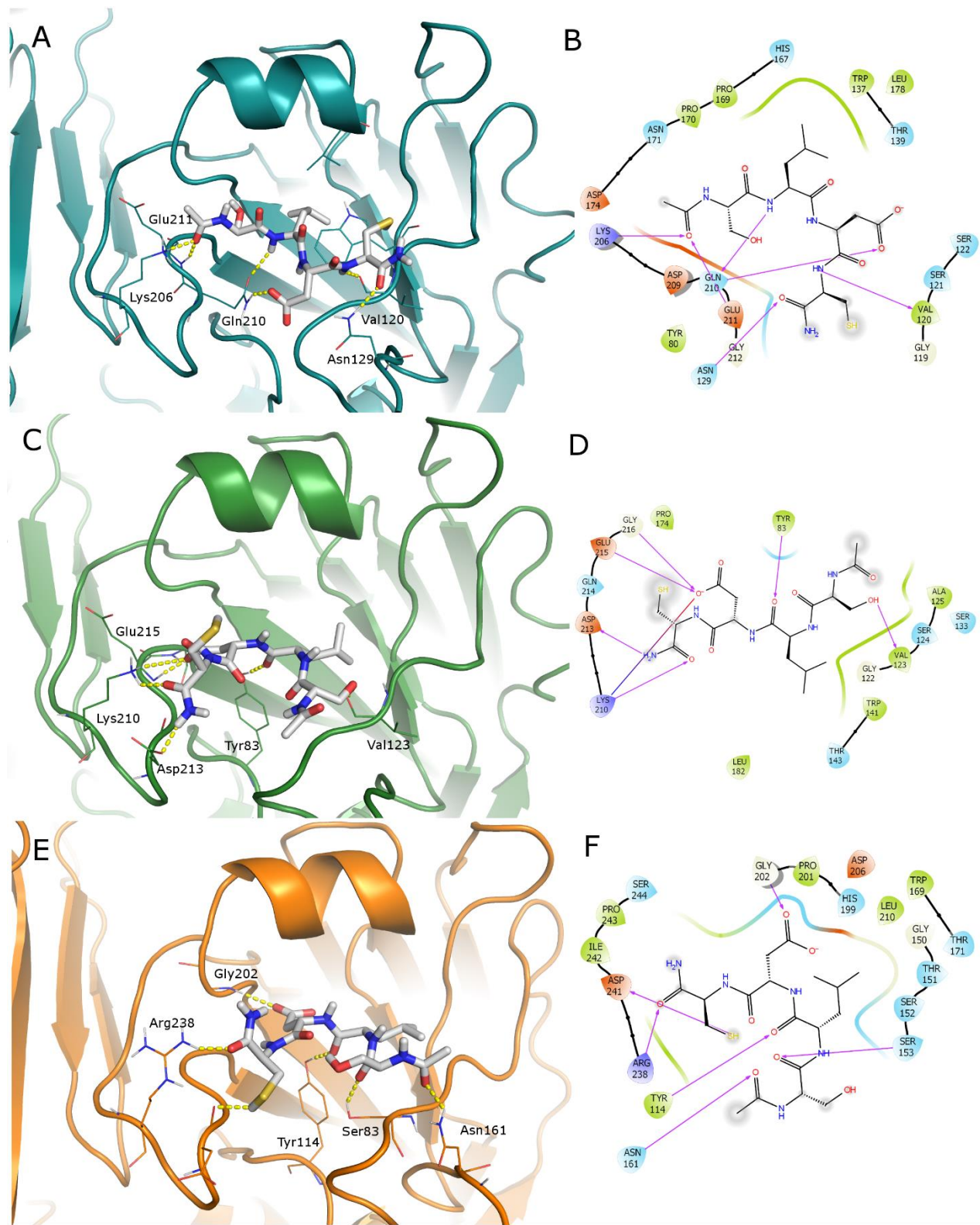


Figure S22. Docked poses of peptide 2 (white C atoms, represented as stick) in the RBS of studied HAs represented as cartoon: A) Parma/H1N1 (deep-cyan); B) Roma/H1N1 (dark green); C) Parma/H3N2 (orange). Residues involved in H-bond interactions with the ligand are represented as lines; H-bond are depicted as yellow dashed lines. Corresponding 2D ligand interaction diagrams are reported in panels B), D) and E); in the diagrams residues close to the ligand are coloured on the basis of their properties (orange, negatively charged; blue, positively charged; green, hydrophobic; cyan, polar), H-bonds are depicted as magenta arrows, solvent exposed atoms are surrounded by a grey shadow.

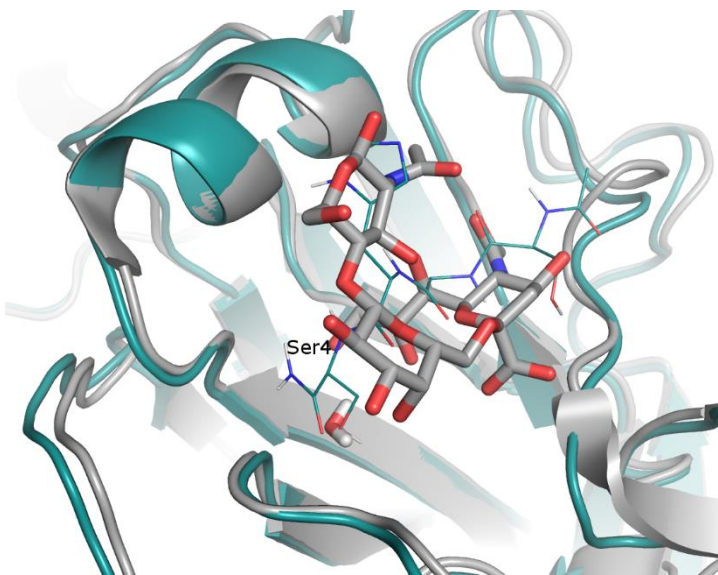


Figure S23. Superposition of the complex of HA:sialic acid (PDB ID 3UBN, grey carbon atoms) with docked pose of SAHS in the A/Parma/24/09 H1N1 (deepcyan carbon atoms). Proteins are represented as cartoon. Sialic acid and conserved water molecule are represented as stick, while the SAHS is represented as thin stick.